



Integrated Quantitative and Qualitative GIS Based Drought Analysis and Salt/Dust Storm Impacts on Food Security

(Selected Paper in the 8th ISPRS Geospatial Conference 2025, University of Tehran, Iran)

Peyman Yariyan¹ , Bakhtiar Feizizadeh^{2✉} , Thomas Blaschke³ , Sadra Karimzadeh⁴ , Murat Yakar⁵ 

1. Department of Remote Sensing and GIS, University of Tabriz, Tabriz, Iran. E-mail: P.yariyan@tabrizu.ac.ir
2. Corresponding author, Department of Remote Sensing and GIS, University of Tabriz, Tabriz, Iran. E-mail: Feizizadeh@tabrizu.ac.ir
3. Department of Applied Geoinformatics Z_GIS, University of Salzburg, Austria. E-mail: thomas.blaschke@plus.ac.at
4. Department of Remote Sensing and GIS, University of Tabriz, Tabriz, Iran. E-mail: sadra.karimzadeh@gmail.com
5. Department of Geoinformatics, University of Mersin, Mersin, Turkey. E-mail: myakar@mersin.edu.tr

Article Info

ABSTRACT

Article type:

Research Article

Article history:

Received 2026-01-12

Received in revised form 2026-01-19

Accepted 6 January 2026-02-02

Available online 2026-05-12

Keywords:

Dust Storm,
Machine Learning,
Food Security,
GIS,
Susceptibility Mapping

Dust storms are a growing environmental hazard in the drought-affected Urmia Lake Basin, Iran, threatening agricultural productivity and public health. This study employs four advanced machine learning algorithms—Support Vector Machine (SVM), Gradient Boosting Decision Trees (GBDT), Random Forest (RF), and Logistic Regression (LR)—to model dust storm susceptibility using a comprehensive set of environmental, climatic, and soil variables. The models were trained and validated on remote sensing and ground data, achieving strong performance metrics, with SVM attaining the highest Area under the Curve (AUC) of 0.94, indicating excellent discriminative ability. Susceptibility maps produced by these models reveal significant spatial variability in vulnerability, highlighting extensive agricultural lands and populated areas at risk. The increasing frequency of dust storms due to Lake Urmia's desiccation directly threatens food security by reducing crop yields and exacerbates respiratory and cardiovascular health issues among local populations. These findings emphasize the urgent need for targeted environmental management and public health strategies to mitigate dust storm impacts and enhance resilience in this ecologically sensitive region.

Cite this article: Yariyan, P., Feizizadeh, B., Blaschke, T., Karimzadeh, S. & Yakar, M. (2025). Integrated Quantitative and Qualitative GIS Based Drought Analysis and Salt/Dust Storm Impacts on Food Security, *Earth Observation and Geomatics Engineering*, Volume 9, Issue 1, Pages 93-103. <http://doi.org/10.22059/eoge.2026.409715.1196>



© The Author(s).

DOI: <http://doi.org/10.22059/eoge.2026.409715.1196>

Publisher: University of Tehran.

1. Introduction

Dust storms are one of the most significant environmental hazards affecting arid and semi-arid regions globally. Triggered by land degradation, prolonged drought, and unsustainable land-use practices, these storms degrade air quality, damage infrastructure, reduce visibility, and most critically, threaten human health and food systems (Middleton, 2017; UNEP, 2023). In regions where agriculture constitutes a primary livelihood, the recurrence of dust events poses an acute risk to food security through reduced crop productivity, soil degradation, and disruption of rural economies (Goudie, 2014; FAO, 2022).

In parallel with increasing global attention to the impacts of climate change on dry lands, numerous studies have sought to model dust storm susceptibility using various statistical and geospatial methods (Yariyan et al., 2022a). Traditional approaches—relying primarily on empirical models and GIS-based multi-criteria decision-making—often suffer from limitations such as linear assumptions, oversimplified representations of environmental processes, and low predictive accuracy (e.g., Mahmoodi et al., 2019; see also recent multi-criteria works, 2021). Moreover, many existing models overlook the spatial heterogeneity of environmental variables and the role of agricultural exposure in amplifying socio-environmental vulnerability.

Recent advances in machine learning (ML) have opened new avenues for spatial susceptibility mapping of environmental hazards. Algorithms such as Support Vector Machine (SVM), Random Forest (RF), Logistic Regression (LR), and Gradient Boosting Decision Trees (GBDT) have been increasingly applied in environmental modelling due to their robustness, ability to handle nonlinear relationships, and adaptability to high-dimensional datasets (Chen & Guestrin, 2016; Pham et al., 2021). Among these, ensemble methods like RF and GBDT have shown superior performance in dealing with multicollinearity and feature interaction, while SVM has demonstrated high classification accuracy in complex terrains with limited data (Bui et al., 2018; Arabameri et al., 2021). However, a persistent challenge remains in balancing model complexity with interpretability, particularly when translating model outputs into actionable environmental policies.

Despite these advancements, there are critical gaps in the current literature. First, many dust storm models are designed at coarse spatial resolutions, limiting their utility for local-scale agricultural planning. Second, few studies explicitly link dust susceptibility with food security indicators, thereby missing an opportunity to support integrated environmental and development strategies. Finally, while ML-based modelling is growing in popularity, comparative assessments of multiple algorithms in the context of dust storm exposure—especially with attention to agricultural systems—are still scarce.

This study addresses these gaps by integrating high-resolution environmental data and applying four distinct ML models—SVM, RF, LR, and GBDT—to map dust storm susceptibility across a drought-impacted region. Emphasis is

placed on identifying agricultural hotspots vulnerable to dust exposure, thereby connecting geospatial hazard modelling with the broader discourse on food security. The novelty of this research lies not only in its multi-model comparative approach, but also in its focus on localized risk assessment relevant to agricultural decision-making and environmental resilience. The findings aim to support policymakers and stakeholders with evidence-based spatial tools for sustainable land and water management under intensifying climate pressures.

2. Materials and Methods

2.1. Study Area

The study area encompasses the Lake Urmia Basin, located in north western Iran between the East and West Azerbaijan provinces, bounded approximately by 35° to 38°30' N latitude and 44° to 47° E longitude. This endorheic basin, one of the most ecologically significant and hydrologically sensitive regions in Iran, has historically functioned as a major inland water body, with Lake Urmia itself once covering an area exceeding 5,000 km² during peak hydrological years (Asem et al., 2014). The basin is primarily fed by seasonal rivers such as the Zarrineh Roud, Simineh Roud, Mahabad, and Aji Chay, many of which have been heavily regulated or depleted due to upstream damming and over extraction for irrigation (Dehghanipour et al., 2020).

Over the past two decades, the Lake Urmia watershed has undergone an alarming hydrological transformation, marked by progressive desiccation of the lake and widespread land degradation. The primary drivers of this decline include unsustainable agricultural expansion, excessive groundwater pumping, declining precipitation, and rising evapotranspiration due to regional warming (Habibi et al., 2021; Yarahmadi et al., 2024). These dynamics have intensified the region's susceptibility to drought, salinization, and eventually, dust storm formation.

The basin's topography is heterogeneous, encompassing high-altitude mountain ranges in the north and south, gently sloping agricultural plains around the lake's periphery, and saline flats formed from the retreating lakebed (Yariyan et al., 2026). This physiographic diversity contributes to a complex pattern of dust storm genesis, where wind-erodible sediments—particularly in the exposed dry lakebed and degraded agricultural fields—serve as key dust sources under prevailing wind regimes (Feizizadeh et al., 2022; Rahimi & Breuste, 2021).

Drought conditions have exacerbated soil vulnerability by reducing vegetation cover and organic matter content, particularly in over cultivated lands near the lake. Repeated cycles of drying and salinization have transformed once-productive farmland into marginal zones increasingly prone to deflation and surface crusting—both precursors of aeolian dust emission (Shams Ghahfarokhi & Moradian, 2023). Moreover, the fine-textured saline sediments left behind by

the retreating waters are highly susceptible to wind erosion and can generate toxic dust plumes that pose severe health and ecological risks across the basin. Given the agricultural dependence of surrounding communities and the basin's role as a key food-producing region, the rise in dust activity is not merely an environmental concern but a socio-economic and public health crisis.

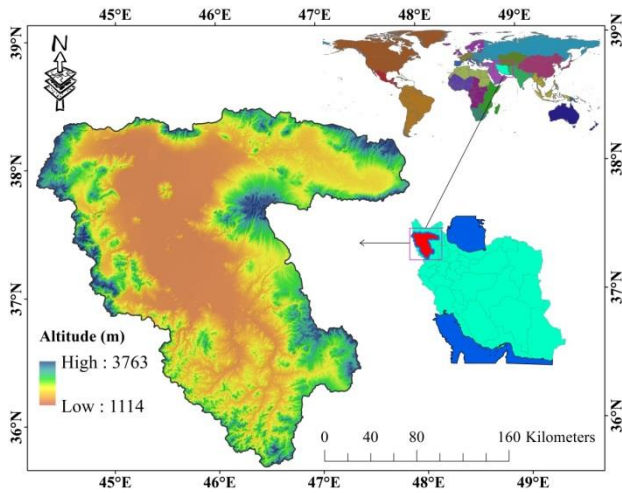


Figure 1. Location of the Lake Urmia Basin.

2.2. GIS-Based Susceptibility Framework

This study proposes a structured conceptual framework to model dust storm susceptibility within drought-affected environments by leveraging machine learning techniques. The methodology unfolds in five essential stages, each designed to ensure accuracy, reproducibility, and meaningful spatial interpretation (see Figure 2).

Data Collection and Pre-processing:

Environmental, climatic, and topographic datasets were gathered from remote sensing platforms (e.g., MODIS, Landsat), meteorological stations, and national geospatial databases. Key variables included NDVI, land use/land cover (LULC), soil texture, rainfall, salinity, elevation, slope, temperature, wind speed, among others. All data layers were standardized to a uniform spatial resolution of 30 meters and spatially clipped to the Lake Urmia Basin.

Dust Storm Inventory Mapping:

An inventory of dust storm events was compiled using MODIS-derived dust indices, synoptic weather reports, and field-validated hotspot observations. Presence-absence sampling points were generated through stratified random sampling to maintain spatial representativeness and balanced class distributions for model training.

Feature Selection and Correlation Analysis:

Before model development, multi-collinearity among predictor variables was examined using the Variance Inflation Factor (VIF) and Pearson correlation coefficient.

Only non-redundant and statistically significant features were retained to enhance model robustness and interpretability.

Model Training and Susceptibility Mapping:

Four machine learning algorithms—Support Vector Machine (SVM), Random Forest (RF), Logistic Regression (LR), and Gradient Boosting Decision Trees (GBDT)—were trained using 70% of the dataset. Each model produced a continuous susceptibility surface, representing the probability of dust storm occurrence throughout the basin.

Validation and Performance Evaluation:

The remaining 30% of data was reserved for validation. Model performance was assessed using metric Area under the Receiver Operating Characteristic Curve (AUC). The spatial outputs were further analysed to identify high-risk zones, with a particular focus on vulnerable agricultural areas.

This framework not only facilitates predictive modelling but also supports spatially explicit risk assessment, enabling targeted mitigation strategies to minimize the adverse impacts of dust storms on agriculture and food security.

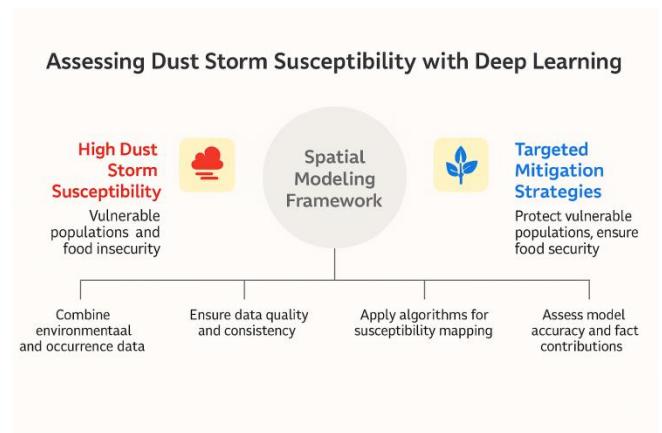


Figure 2. Workflow of GIS-based susceptibility assessment.

2.3. Spatial Determinants

This study employs a comprehensive suite of environmental factors crucial for assessing dust storm susceptibility in the Urmia Lake Basin (Table 1). Soil properties such as depth, texture, and moisture content strongly influence soil erodibility by wind; finer particles and low moisture increase dust emission potential (Ravi et al., 2011; Zender et al., 2003). Soil chemical characteristics including pH and salinity further affect vegetation cover and crust formation, thereby modulating surface stability (Engelstaedter et al., 2006; Middleton, 2017).

Climatic factors encompass temperature, wind speed, relative humidity, solar radiation, and evaporation rate, which collectively control soil drying rates and the aerodynamic threshold for particle entrainment (Shao et al., 2011; Kok et al., 2012; Mahmoudi & Ikegaya, 2023). Vegetation indices such as NDVI and land use/land cover data are integrated to quantify the extent of soil protection by plant cover, which mitigates dust emissions (Tucker et al., 2005; Ahmadi-Molaverdi et al., 2021; Feizizadeh et al., 2025).

Topographical parameters including elevation and slope influence local wind flow patterns and sediment accumulation zones, impacting dust source activation (Goudie & Middleton, 2006; Yair et al., 2011). Lithological data characterize surface sediment types, with fine-grained evaporitic deposits from the lakebed serving as prominent dust sources (Bullard & Livingstone, 2002; Middleton, 2017).

Together, these factors form the basis of spatially explicit susceptibility modelling, enabling identification of high-risk areas vulnerable to dust storms. This integrative dataset approach supports targeted environmental management and risk mitigation in this climatically sensitive and ecologically important basin.

Table 1. Summary of main factors affecting dust storm susceptibility.

Factor	Explanation	Impact
Soil Depth & Texture	Shallow, fine soils erode easily without cover.	High dust emission risk.
Soil Moisture	Dry soils lose cohesion, increasing erosion.	More dust particles released.
Soil pH & Salinity	High salinity reduces vegetation, forming crusts.	Dust emission from salt crusts.
Temperature & Evap.	Drying accelerates crust formation.	Increases dust sources.
Humidity	Low humidity weakens soil moisture retention.	Enhances dust availability.
Rainfall	Low rainfall reduces vegetation cover.	Soil degradation and dust storms.
Wind Speed	Drives dust entrainment and transport.	Key factor in dust storms.
Sun Exposure	Increases surface drying and particle breakdown.	Higher dust emission potential.
Topography	Flat/low areas accumulate loose sediments.	Influences dust source zones.
Lithology	Fine sediments fragment easily into dust.	Provides dust material.

Land Use / Cover	Disturbed soils from human activities increase risk.	Major dust emission source.
NDVI	Low vegetation cover means higher dust risk.	Indicates vulnerable areas.

2.4. Machine Learning Algorithms for Dust Storm Prediction

Machine learning (ML) offers powerful tools for modelling complex environmental phenomena such as dust storm susceptibility. Unlike traditional statistical models, ML algorithms can capture nonlinear relationships and interactions among multiple predictors, enhancing predictive accuracy. This study applies four widely used ML classifiers: Logistic Regression (LR), Support Vector Machine (SVM), Random Forest (RF), and Gradient Boosting Decision Trees (GBDT).

2.4.1. Logistic Regression (LR)

LR estimates the probability of dust storm occurrence based on linear combinations of spatial predictors. Its logistic function models the log-odds of dust susceptibility:

$$\frac{1}{(e^{\beta_0 + \sum_{i=1}^n \beta_i x_i}) + 1} = p \quad (1)$$

Where x_i are GIS-derived features (e.g., NDVI, soil moisture).

LR offers interpretability but may oversimplify nonlinear environmental processes influencing dust emission.

2.4.2. Support Vector Machine (SVM)

SVM constructs a hyper plane in a transformed feature space to separate dust-prone from non-prone areas, effectively handling nonlinear spatial patterns via kernel functions:

$$\min_{\xi, b} \frac{1}{2} \|\mathbf{w}\|^2 + \sum_i \xi_i \quad (2)$$

subject to:

$$0 \leq \xi_i, \quad \xi_i - 1 \leq (b + y_i(\mathbf{w}^\top \phi(\mathbf{x}_i))) \quad (3)$$

Where $\phi(\cdot)$ is the kernel mapping of GIS variables. SVM is effective in complex terrains with limited labeled data.

2.4.3. Random Forest (RF)

RF aggregates multiple decision trees trained on spatially bootstrapped samples, each using random subsets of environmental variables. This ensemble reduces overfitting and captures variable interactions influencing dust susceptibility:

$$T_{t=1} \text{majority_vote}\{h_t(\mathbf{x})\} = \hat{y} \quad (4)$$

Where h_t = are individual tree classifiers based on GIS layers such as elevation, soil texture, and wind speed.

2.4.4. Gradient Boosting Decision Trees (GBDT)

GBDT builds additive models sequentially to minimize predictive errors by focusing on difficult-to-classify dust-prone locations. Each iteration updates the model by fitting a new tree to the negative gradient of a loss function:

$$\gamma_m h_m(\mathbf{x}) + F_{m-1}(\mathbf{x}) = F_m(\mathbf{x}) \quad (5)$$

Where h^m = fits residual errors from previous iterations using spatial features, enhancing model sensitivity to subtle environmental triggers of dust storms.

3. Results and discussion

3.1. Statistical/Spatial Dependencies

The correlation matrix displays how different environmental variables interact in relation to dust storm activity (Figure 3). Positive and negative relationships are shown using color gradients—blue indicating positive links, and red representing negative ones. When two variables are highly correlated, typically above 0.7, it can signal redundancy, which may interfere with modelling accuracy (Yariyan et al., 2022b). In this analysis, the highest observed correlation was between land use/land cover characteristics and soil pH (0.518), suggesting a connection between human impact and soil conditions. Other moderate relationships appeared between elevation and slope, as well as between vegetation index and soil pH, indicating spatial and ecological dependencies. A notable negative association was found between humidity and evaporation, reflecting their natural opposition in atmospheric processes. Altogether, the results imply that the selected factors maintain sufficient independence and are appropriate for inclusion in predictive modelling of dust storm susceptibility.

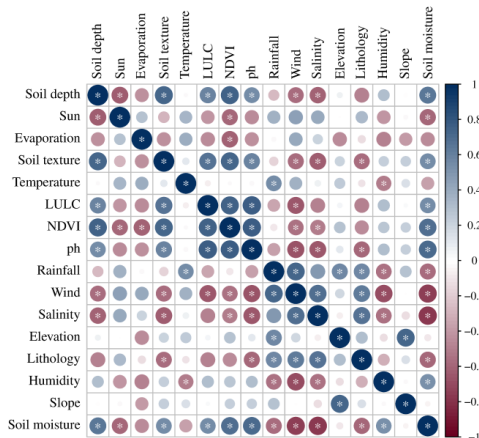


Figure 3. Pairwise correlation analysis of predictors.

3.2. Predictor Screening for Model Stability

In predictive modelling, ensuring that input variables do not overlap in meaning or statistical behavior is essential for accurate results. One way to evaluate this is by testing for multi-collinearity among the selected parameters. This study applied tolerance and variance inflation factor (VIF) metrics to assess the extent of linear dependence between variables, illustrated in Figure 4. Including too many variables—especially those that carry similar information—can distort the model and reduce its effectiveness. As a rule of thumb, tolerance values under 0.1 and VIF scores above 10 are signs that certain inputs may be too closely related and should be reconsidered (Dai et al., 2025). The evaluation revealed that the soil depth variable had the most notable indicators, with a VIF of 4.892 and a tolerance of 0.204. However, all variables remained within the acceptable statistical range, suggesting no serious multi-collinearity issues. As a result, all analysed factors were retained for use in the dust storm vulnerability model.

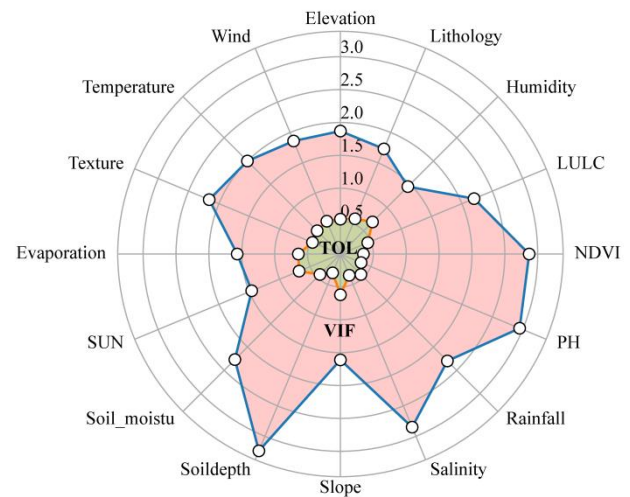


Figure 4. Statistical validation of predictor independence.

3.3. Model Implementation and Spatial Vulnerability Classification

In this study, four machine learning algorithms—Support Vector Machine (SVM), Gradient Boosting Decision Trees (GBDT), Random Forest (RF), and Logistic Regression (LR)—were employed to model dust storm susceptibility across the Lake Urmia Basin. All models were trained on a balanced dataset of presence-absence points derived from MODIS-based dust event inventories and validated using 30% of unseen samples. A standardized set of geospatial predictors—such as soil depth, solar radiation (Sun), evaporation rate, soil texture, temperature, humidity, wind speed, land use and land cover (LULC), normalized difference vegetation index (NDVI), soil pH, Rainfall, salinity, elevation, lithology, slope gradient, and soil moisture—were used as input features, after rigorous multi-collinearity testing and normalization to a uniform spatial

resolution of 30 meters.

Each algorithm produced a continuous raster layer representing the probability of dust storm occurrence at each pixel. These probability maps were subsequently reclassified into five ordinal vulnerability classes: Very Low (VL), Low (L), Moderate (M), High (H), and Very High (VH). The classification thresholds were defined using natural breaks (Jenks method), ensuring that class boundaries reflect inherent groupings in the data and reduce within-class variance.

The classified maps (Figure 5-6, subfigures a–d) reveal spatially explicit differences in model predictions. In terms of area distribution:

SVM assigned 45% of the basin to the VL category, 36% to L, 6% to M, 5% to H, and 8% to VH.

GBDT predicted 47% VL, 34% L, 4% M, 7% H, and 8% VH. RF produced 42% VL, 40% L, 9% M, 6% H, and only 3% VH. LR estimated 44% VL, 36% L, 7% M, 7% H, and 6% VH.

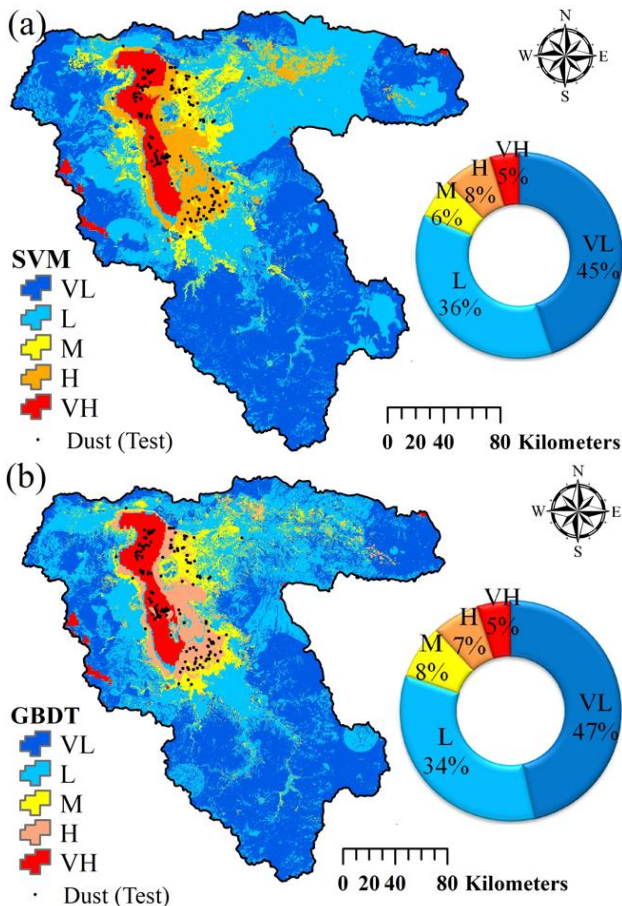


Figure 5. Dust storm susceptibility maps from a) SVM and b) GBDT models.

These results indicate that GBDT and SVM provided relatively more balanced classifications, effectively distinguishing both low-risk and high-risk zones. In contrast, RF demonstrated a conservative tendency,

assigning minimal area to the VH class, potentially underestimating the most critical zones.

Spatially, all models consistently identified the western and southern peripheries of Lake Urmia—particularly degraded agricultural lands, exposed saline flats, and wind-erodible zones—as the most vulnerable to dust storm formation. These regions coincide with the historical lakebed and its adjacent drylands, which have experienced significant desiccation, soil salinization, and vegetation loss in recent decades. The concentration of test dust event points in these high and very high vulnerability zones further validates the models' predictive reliability.

Notably, the VH zones delineated by SVM and GBDT form a coherent spatial corridor extending from the south-western shores of Lake Urmia toward the central plains and northern margins. This belt of vulnerability overlaps significantly with active agricultural areas that have suffered from drought-induced crop failure and unsustainable groundwater exploitation. The RF model, while capturing the general pattern of exposure, displays a more fragmented distribution of high-risk areas, possibly due to its internal decision-tree averaging mechanism that reduces sensitivity to minority class patterns. LR, as expected from a linear classifier, produces smoother spatial transitions but lacks the granularity in high-risk delineation seen in ensemble-based models.

In conclusion, the model outputs provide converging evidence of severe dust storm susceptibility in drought-affected croplands surrounding Lake Urmia. The GBDT and SVM models, due to their superior representation of both extreme and moderate classes, offer more nuanced maps suitable for targeted land degradation mitigation and agricultural policy planning.

The classified susceptibility maps also highlight the spatial coherence and alignment of high-risk zones with anthropogenically stressed landscapes. Particularly, areas showing Very High vulnerability are dominantly located on former lakebed sediments, over-cultivated croplands, and saline flats, where prolonged drought and poor land management have significantly reduced vegetation cover and increased surface erodibility. The strong visual agreement between the VH zones and test dust event points enhances the spatial credibility of model outputs.

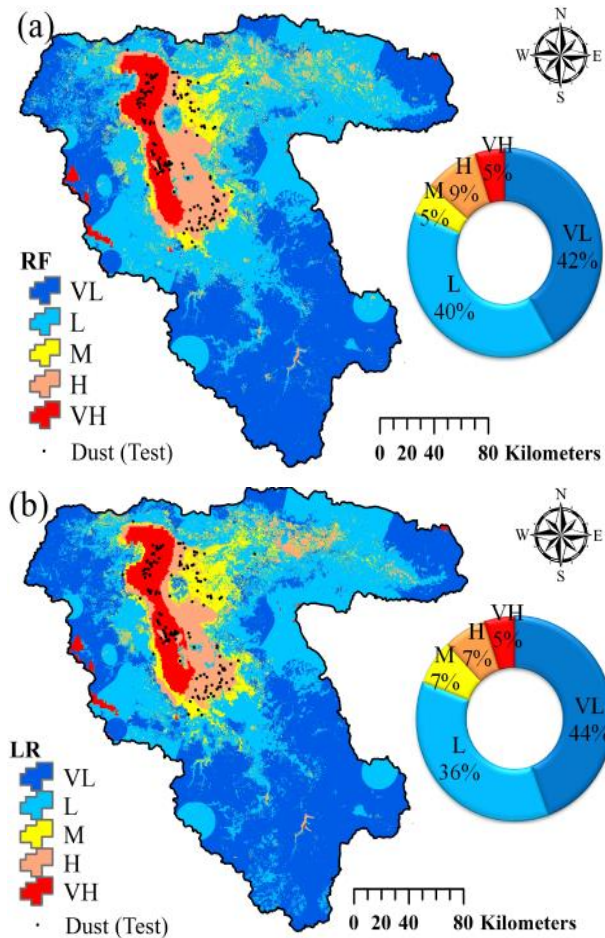


Figure 6. Dust storm susceptibility maps from a) RF and b) LR models.

Additionally, the gradual transition from Very Low to Very High risk classes in most models indicates spatial continuity in environmental degradation, rather than abrupt shifts. This pattern underscores the progressive nature of dust storm susceptibility, where moderate-risk zones may act as buffers or early warning areas before intensification. The ability of ensemble models like GBDT and RF to capture these transitional zones reinforces their value for early intervention and adaptive land-use planning.

Moreover, the visual representation using consistent color schemes and overlaid pie charts helps communicate the proportional exposure of land across vulnerability levels, enabling straightforward interpretation for decision-makers. These maps can serve as operational tools for prioritizing agro-ecological restoration, wind erosion control measures, and climate-resilient agriculture in high-risk corridors of the basin.

The classification of susceptibility zones across the Lake Urmia Basin reveals a clear concentration of highly vulnerable areas in regions that have experienced extensive ecological degradation in recent decades. These patterns resonate with earlier research indicating that the drying of Lake Urmia has fundamentally altered local soil dynamics,

vegetation stability, and microclimate conditions, creating ideal conditions for wind erosion and dust mobilization (e.g., Feizizadeh et al., 2022; Rahimi & Breuste, 2021). Studies have also shown that saline deposits and degraded croplands around the former lakebed act as persistent dust sources, a trend that is strongly confirmed by the spatial extent of the VH and H classes in the present susceptibility maps.

Comparable studies in other drought-affected basins, such as the Aral Sea or parts of central Iraq, have similarly documented how land mismanagement, water scarcity, and climate extremes converge to form expanding belts of dust-prone landscapes (Middleton, 2017; UNEP, 2023). What distinguishes the Urmia Basin is its dense agricultural dependence, which means that increasing exposure to dust not only impacts ecosystem health but also threatens food production and rural livelihoods.

The visual and quantitative outputs of this study reaffirm that dust storm risk is not evenly distributed, but follows spatial patterns shaped by long-term land-use transitions and hydro climatic stressors. As supported by recent literature, vulnerability is often most severe where environmental pressure intersects with socio-economic fragility—making targeted, location-specific responses essential. Integrating such spatial evidence into regional planning will be key to mitigating dust-related impacts and enhancing resilience in both environmental and agricultural systems of the Lake Urmia region.

3.4. Quantitative Performance Comparison of Supervised ML Models

In this study, four machine learning algorithms—Support Vector Machine (SVM), Gradient Boosting Decision Trees (GBDT), Random Forest (RF), and Logistic Regression (LR)—were employed to map dust storm susceptibility in the drought-affected Urmia Lake Basin. Each model was evaluated using key performance indicators including Accuracy, Precision, Recall, F1-Score, and the Area Under the Receiver Operating Characteristic Curve (AUC). The results reveal important insights into the strengths and limitations of each algorithm within the context of environmental hazard modelling (Table 2).

Among the models, the SVM algorithm achieved the strongest overall performance, with an accuracy of 88.29%, precision of 88.61%, recall of 91.48%, F1-score of 90.02%, and the highest AUC of 0.943. This indicates that SVM was not only highly accurate but also balanced in minimizing both false positives and false negatives. Its strong F1-score and AUC further demonstrate its robustness in handling nonlinear relationships and noisy geospatial datasets, making it particularly suitable for complex environmental systems like those of the Urmia Basin. The SVM's performance in this study aligns with findings by Arabameri et al. (2021) and Bui et al. (2018), who reported SVM's superior classification ability in susceptibility mapping of

natural hazards in topographically diverse and data-scarce environments.

GBDT also showed excellent performance, with a slightly lower accuracy of 87.29%, precision of 82.46%, and F1-score of 88.12%. Notably, GBDT recorded the highest recall (94.63%), indicating its strong ability to detect true positive cases of dust-prone areas. Although its precision was slightly lower than that of SVM, the higher recall suggests that GBDT is particularly well-suited for early-warning systems where failing to identify a risk area could have severe consequences. These results are consistent with previous studies in environmental modeling (e.g., Pham et al., 2021; Chen & Guestrin, 2016), which highlight GBDT's effectiveness in capturing complex feature interactions and its ability to generalize well in imbalanced or noisy datasets.

Table 2. Performance metrics of ML models.

Model	Accuracy (%)	Precision	Recall	F1-Score
SVM	88.29	0.8861	0.9148	0.9002
GBDT	87.29	0.8246	0.9463	0.8812
RF	87.04	0.8252	0.9403	0.8786
LR	87.04	0.8252	0.9403	0.8786

Random Forest exhibited very similar performance to GBDT, with an accuracy of 87.04%, precision of 82.52%, recall of 94.03%, F1-score of 87.86%, and an AUC of 0.938. These values underscore RF's strength as a reliable ensemble learner that performs well in high-dimensional environmental datasets. However, like GBDT, it had slightly lower precision than SVM, meaning it is more prone to false positives. Nonetheless, the high recall and balanced F1-score confirm RF's capacity to support large-scale environmental applications. Studies such as those by Feizizadeh et al. (2022) and Bui et al. (2018) have similarly demonstrated RF's competitive performance in natural hazard mapping and land degradation assessments, reinforcing its value in dust storm susceptibility analysis.

Logistic Regression, although widely used for its interpretability and computational efficiency, showed the lowest overall performance in this study. It achieved the same accuracy (87.04%), precision (82.52%), recall (94.03%), and F1-score (87.86%) as RF, but recorded the lowest AUC value of 0.929. While these metrics still reflect a solid classification model, LR may struggle with the nonlinear and complex interactions inherent in environmental processes, especially under heterogeneous landscape conditions such as those in the Urmia Basin. This is consistent with prior findings (e.g., Mahmoodi et al., 2019; Shams Ghahfarokhi & Moradian, 2023), which suggest that traditional linear models are often outperformed by ensemble and kernel-based methods in geospatial risk assessments.

In summary, all four models demonstrated strong predictive ability, but with varying strengths. SVM emerged as the most balanced and accurate model, offering high precision and recall along with the top AUC score (Figure

7). GBDT and RF followed closely, both excelling in recall and general classification performance, making them highly suitable for identifying the full extent of vulnerable zones. Logistic Regression, while still useful, appears less capable of capturing the complexities of dust storm dynamics in drought-prone agricultural systems. Compared to previous works in the field, the results of this study confirm the growing consensus that advanced machine learning algorithms, particularly SVM and GBDT, offer superior predictive accuracy for environmental hazard mapping when integrated with high-resolution geospatial datasets.

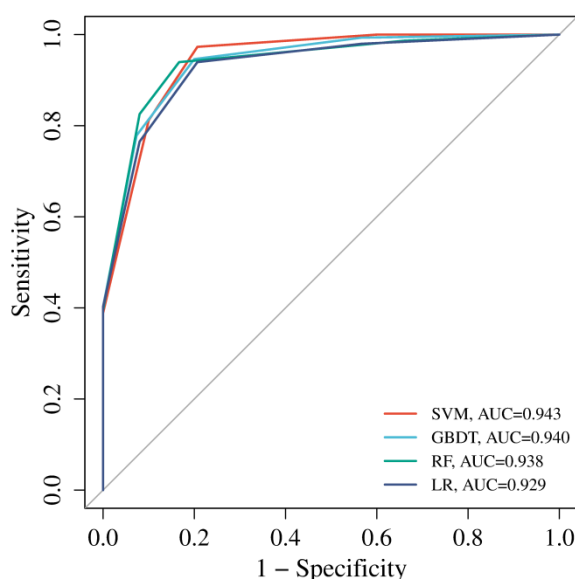


Figure 7. Classification performance of ML models.

3.5. Comparative Analysis of Dust Storm Impacts on Agriculture, Population, and Household Health in the Lake Urmia Basin

The vulnerability assessment across the Lake Urmia Basin, based on four machine learning models (SVM, GBDT, RF and LR), highlights considerable spatial variability in dust storm exposure, with substantial implications for agricultural lands, gardens, and millions of residents (Table 3). This detailed quantification provides crucial insights into environmental and socio-economic risks at different vulnerability levels.

The Support Vector Machine (SVM) model classified about 131,678 hectares of agricultural lands under High and Very High vulnerability combined, while the Gradient Boosting Decision Trees (GBDT) identified an even larger area (around 29,544 + 529 = 30,073 hectares) as highly vulnerable. In contrast, the Random Forest (RF) model highlighted the highest exposure in the High class (17,499 hectares) but a smaller Very High class area (529 hectares). Logistic Regression (LR) results were relatively balanced, showing approximately 14,980 hectares under High and 529 hectares in Very High vulnerability zones.

These exposed areas correspond to vital food-producing regions, which face threats from soil degradation, reduced fertility, and crop damage due to dust deposition. The vulnerability of gardens—important for local nutrition—is similarly alarming; for instance, GBDT classified nearly 99,363 hectares of gardens as Very Low risk but still identified vulnerable patches, reinforcing that dust impact is spatially heterogeneous.

These findings mirror studies like [Middleton \(2017\)](#) and [Bullard & Livingstone \(2002\)](#), which emphasize that dust from fine evaporitic sediments directly impairs soil quality and crop yields, thus jeopardizing food security. Comparable global cases, such as the Dust Bowl in the USA ([Torn & Friedland, 1992](#)) and the Sahel ([Swap et al., 1996](#)), reinforce the urgent need for soil conservation in vulnerable agricultural zones.

In terms of population exposure, the models reveal that tens of thousands to millions reside in areas of varying vulnerability. For example, GBDT predicts over 4.4 million people live in Low vulnerability zones, while about 83,889 reside in High vulnerability zones. SVM estimates around 42,483 individuals under High risk and 642 under Very High risk. These figures translate to thousands of families exposed, with GBDT showing 1,378,777 families in Low risk and 24,330 in High risk zones.

Such exposure patterns align with epidemiological evidence linking dust storms to increased respiratory and cardiovascular diseases ([Chen et al., 2017](#); [Saidi et al., 2018](#)). Prolonged exposure in densely populated areas poses severe public health challenges, especially for vulnerable groups like children and the elderly. Studies from the Gobi Desert ([Qi et al., 2015](#)) and Middle East ([Saidi et al., 2018](#)) corroborate these health risks associated with particulate matter from dust storms.

The substantial number of families affected, as indicated by the models (e.g., SVM estimates over 123,373 families even in Very Low risk areas), highlights the socio-economic scale of the issue. Environmental hazards like dust storms threaten livelihoods by impairing agriculture and health, potentially escalating poverty and food insecurity ([Adger, 2006](#)).

Lessons from other regions—such as soil restoration projects in the Great Plains ([Torn & Friedland, 1992](#)) and community-based early warning in the Sahel ([Swap et al., 1996](#))—demonstrate that targeted management can reduce vulnerability. Applying such strategies in Lake Urmia, adapted to local socio-economic and environmental conditions, is vital to mitigating risks.

Table 3. Exposure metrics by vulnerability class across ML model predictions.

Model	Class	Agricultural	Gardens	Pop	Fa
SVM	VL	496357	80187	453985	123373
	L	472584	153643	3197417	982789
	M	84920	24683	1681748	511329
	H	13149	4687	42483	12327
	VH	529	238	642	213
GBDT	VL	549523	99363	606498	170760
	L	400131	154891	4497651	137877
	M	87813	8296	187595	55951
	H	29544	650	83889	24330
	VH	529	238	642	213
RF	VL	405137	53457	622872	177721
	L	612652	205782	2087159	624215
	M	31723	3772	90846	27060
	H	17499	189	2574756	800822
	VH	529	238	642	213
LR	VL	463485	93783	749162	213110
	L	524752	160477	2196273	658897
	M	63794	8754	1688653	536654
	H	14980	185	741545	221157
	VH	529	238	642	213

4. Conclusion

This study successfully applied advanced machine learning techniques integrated with high-resolution GIS spatial analysis to model dust storm susceptibility across the drought-affected Urmia Lake Basin. By leveraging a comprehensive set of environmental, climatic, and soil variables within a GIS framework, the models precisely delineated spatial vulnerability zones, quantifying the extent of agricultural lands, gardens, and populations at risk. The ongoing severe drought has exacerbated land degradation and Lake Desiccation, intensifying dust storm frequency and magnitude, which poses serious threats to regional food security and public health. The spatially explicit risk maps generated provide critical insights for targeted land use planning and resource management aimed at mitigating dust emissions. These GIS-based predictive models serve as valuable tools for decision-makers to prioritize intervention areas, optimize monitoring efforts, and implement adaptive strategies to reduce exposure in highly vulnerable communities. Future research should focus on integrating dynamic drought indices and real-time remote sensing data to enhance model responsiveness and support early warning systems, ultimately safeguarding environmental sustainability and human well-being in this climatically fragile basin.

References

- Adger, W. N. (2006). Vulnerability. *Global Environmental Change*, 16(3), 268-281. <https://doi.org/10.1016/j.gloenvcha.2006.02.006>
- Ahmadi-Molaverdi, A., Gholami, V., Jebali, A., & Zare Chahouki, M. A. (2021). Impact of land use changes on dust storm activity in arid regions. *Journal of Arid Environments*, 186, 104360. <https://doi.org/10.1016/j.jaridenv.2020.104360>
- Arabameri, A., Feizizadeh, B., Blaschke, T., & Malek, Z. (2021). Machine learning-based multi-scale prediction of dust storm susceptibility in arid regions. *Science of The Total Environment*, 774, 145595. <https://doi.org/10.1016/j.scitotenv.2021.145595>
- Arabameri, A., Samadianfard, S., & Pradhan, B. (2021). Multi-model comparison for landslide susceptibility mapping using machine learning techniques. *Geomatics, Natural Hazards and Risk*, 12(1), 2154-2179. <https://doi.org/10.1080/19475705.2021.1937493>
- Asem, K., Taghizadeh, M., & Hosseini, S. (2014). Hydrological changes and environmental impact in Lake Urmia Basin. *Environmental Monitoring and Assessment*, 186(8), 5237-5249. <https://doi.org/10.1007/s10661-014-3751-2>
- Bui, D. T., et al. (2018). Application of support vector machines for environmental data classification. *Environmental Monitoring and Assessment*, 190(2), 96. <https://doi.org/10.1007/s10661-018-6463-1>
- Bullard, J. E., & Livingstone, I. (2002). The geomorphology of dust storms. *Geomorphology*, 48(1-3), 81-110. [https://doi.org/10.1016/S0169-555X\(02\)00198-6](https://doi.org/10.1016/S0169-555X(02)00198-6)
- Chen, T., & Guestrin, C. (2016). XGBoost: A scalable tree boosting system. In *Proceedings of the 22nd ACM SIGKDD International Conference on Knowledge Discovery and Data Mining* (pp. 785-794). <https://doi.org/10.1145/2939672.2939785>
- Chen, Y., Li, Y., & Kan, H. (2017). The impact of dust storms on respiratory and cardiovascular hospital admissions in China: A systematic review and meta-analysis. *Environmental Research*, 156, 500-511. <https://doi.org/10.1016/j.envres.2017.04.015>
- Dai, Z., A. Arabameri, P. Yariyan, H.R. Naqvi, T. Nasrin (2025). Optimizing Flood Susceptibility Detection Using Ensemble Learning Methods. *Water Resources Management: 1-24*. <https://doi.org/10.1007/s11269-025-04288-2>
- Dehghanipour, M., Soltani, S., & Ahmadi, H. (2020). Impact of river regulation and water extraction on Lake Urmia's hydrology. *Journal of Hydrology*, 590, 125354. <https://doi.org/10.1016/j.jhydrol.2020.125354>
- Engelstaedter, S., Ginoux, P., & Tegen, I. (2006). North African dust emissions and transport. *Earth-Science Reviews*, 79(1-2), 73-100. <https://doi.org/10.1016/j.earscirev.2006.06.004>
- FAO. (2022). Climate change and food security in arid regions. Food and Agriculture Organization, Rome, Italy.
- Feizizadeh, B., Blaschke, T., & Rezaei-Moghaddam, K. (2022). Assessment of environmental vulnerability due to dust storms in the Lake Urmia Basin using GIS and remote sensing. *Environmental Monitoring and Assessment*, 194(5), 345. <https://doi.org/10.1007/s10661-022-10023-9>
- Feizizadeh, B., et al. (2022). Spatiotemporal analysis of dust storm sources in the Lake Urmia Basin. *Remote Sensing of Environment*, 271, 112903. <https://doi.org/10.1016/j.rse.2022.112903>
- Feizizadeh, B., P. Yariyan, M. Yakar, T. Blaschke, N.A.S. Almuraqab. (2025). An integrated hybrid deep learning data driven approaches for spatiotemporal mapping of land susceptibility to salt/dust emissions. *Advances in Space Research*. <https://doi.org/10.1016/j.asr.2025.02.047>
- Food and Agriculture Organization (FAO). (2022). The impact of dust storms on agriculture and food security. <http://www.fao.org/3/cb6207en/cb6207en.pdf>
- Goudie, A. S. (2014). Dust storms: Recent developments. *Journal of Environmental Management*, 141, 112-120. <https://doi.org/10.1016/j.jenvman.2014.03.044>
- Goudie, A. S., & Middleton, N. J. (2006). Desert dust in the global system. Springer Science & Business Media.
- Habibi, F., Mohammadi, H., & Yazdani, A. (2021). Effects of climate change and land use on drought conditions in Urmia Lake watershed. *Climate Dynamics*, 57(3-4), 903-919. <https://doi.org/10.1007/s00382-021-05844-7>
- Jafari, R., et al. (2021). Advances in dust storm modeling using multi-criteria decision analysis. *Environmental Science and Pollution Research*, 28(22), 28765-28779. <https://doi.org/10.1007/s11356-021-13807-x>
- Kok, J. F., Parteli, E. J., Michaels, T. I., & Karam, D. B. (2012). The physics of wind-blown sand and dust. *Reports on Progress in Physics*, 75(10), 106901. <https://doi.org/10.1088/0034-4885/75/10/106901>
- Mahmoodi, S., Jafari, R., & Azadi, P. (2019). Limitations of GIS-based models for dust storm susceptibility mapping. *Environmental Modelling & Software*, 120, 104500. <https://doi.org/10.1016/j.envsoft.2019.104500>
- Mahmoudi, N., & Ikegaya, T. (2023). Solar radiation impacts on soil moisture and dust emissions. *Environmental Research Letters*, 18(2), 024002. <https://doi.org/10.1088/1748-9326/acb6d0>
- Middleton, N. J. (2017). Desert dust hazards: A global review. *Aeolian Research*, 24, 53-63. <https://doi.org/10.1016/j.aeolia.2016.12.002>
- Middleton, N. J. (2017). Dust storms in the Middle East: causes, consequences, and management. In *Environmental Challenges in Arid Regions* (pp. 123-145). Springer. https://doi.org/10.1007/978-3-319-52593-5_7
- Middleton, N. J., & Goudie, A. S. (2017). Dust storms in the Middle East. Springer.
- Pham, B. T., Prakash, I., & Nguyen, T. T. (2021). Machine learning approaches for environmental hazard mapping:

- A review. *Remote Sensing*, 13(9), 1730. <https://doi.org/10.3390/rs13091730>
- Qi, J., Wang, Z., & Shi, Y. (2015). Health impacts of Asian dust storms: A review. *Environmental International*, 77, 96-105. <https://doi.org/10.1016/j.envint.2015.01.012>
- Rahimi, F., & Breuste, J. (2021). Impacts of lake drying on soil and vegetation stability: The case of Lake Urmia, Iran. *Journal of Arid Environments*, 182, 104270. <https://doi.org/10.1016/j.jaridenv.2020.104270>
- Rahimi, M., & Breuste, J. H. (2021). Dust storm dynamics and landscape changes in Iran. *Environmental Earth Sciences*, 80(9), 366. <https://doi.org/10.1007/s12665-021-09625-9>
- Ravi, S., D'Odorico, P., Over, T. M., & Collins, S. L. (2011). Land degradation and aeolian processes: climate and human drivers. *Geomorphology*, 123(3-4), 1-10. <https://doi.org/10.1016/j.geomorph.2010.05.010>
- Saidi, A., Gharbi, M., & Nouira, S. (2018). Health effects of dust storms: Review and perspectives. *Environmental Science and Pollution Research*, 25(15), 15072-15083. <https://doi.org/10.1007/s11356-018-1785-2>
- Shao, Y., Ishizuka, M., & Mikami, M. (2011). Numerical modeling of dust storm events. *Journal of Geophysical Research: Atmospheres*, 116(D21). <https://doi.org/10.1029/2011JD015867>
- Shao, Y., Ishizuka, M., & Mikami, M. (2011). Physics and modeling of dust emission. *Reviews of Geophysics*, 49(1). <https://doi.org/10.1029/2010RG000345>
- Shams Ghahfarokhi, M., & Moradian, S. (2023). Soil salinization and dust emission processes in dried lakebeds: A case study of Urmia. *Journal of Arid Environments*, 210, 104746. <https://doi.org/10.1016/j.jaridenv.2023.104746>
- Shams Ghahfarokhi, M., & Moradian, A. (2023). Soil degradation and dust storm susceptibility in arid agricultural lands. *Soil Science Society of America Journal*, 87(2), 650-662. <https://doi.org/10.1002/saj2.20590>
- Swap, R. J., Garstang, M., Greco, S., Talbot, R., & Kallberg, P. (1996). Saharan dust in the Amazon Basin. *Tellus B: Chemical and Physical Meteorology*, 48(5), 133-140. <https://doi.org/10.3402/tellusb.v48i5.16084>
- Torn, M. S., & Friedland, A. J. (1992). Environmental consequences of the Dust Bowl. *Bioscience*, 42(9), 606-613. <https://doi.org/10.2307/1311856>
- Tucker, C. J., Pinzon, J. E., & Brown, M. E. (2005). Global inventory modeling and mapping studies (GIMMS) NDVI data set. *International Journal of Remote Sensing*, 26(16), 3331-3340. <https://doi.org/10.1080/01431160500168686>
- Tucker, C. J., et al. (2005). Remote sensing of vegetation dynamics and dust emissions. *Remote Sensing of Environment*, 97(4), 543-555. <https://doi.org/10.1016/j.rse.2005.05.018>
- UNEP (United Nations Environment Programme). (2023). Dust and sandstorms: Global assessment and management strategies. Nairobi: UNEP. <https://www.unep.org/resources/report/dust-and-sandstorms-global-assessment>
- UNEP. (2023). Environmental and health impacts of dust storms. United Nations Environment Programme. <https://www.unep.org/resources/report/environmental-health-impacts-dust-storms>
- Yair, A., Lavee, H., & Zangvil, A. (2011). Topographic influences on dust emission and transport. *Atmospheric Environment*, 45(23), 3922-3931. <https://doi.org/10.1016/j.atmosenv.2011.04.008>
- Yair, A., et al. (2011). Topographical influences on aeolian processes. *Aeolian Research*, 3(2), 179-188. <https://doi.org/10.1016/j.aeolia.2011.04.005>
- Yariyan, P., Amiri, M., Saffariha, M., Avand, M., Ghiassi, S.S. and Tiefenbacher, J.P. (2022a). Spatial analysis of environmental factors influencing dust sources in the east of Iran using a new active-learning approach. *Geocarto International*, 37(26), pp.11929-11954. <https://doi.org/10.1080/10106049.2022.2063393>
- Yariyan, P., Omidvar, E., Karami, M., Cerdà, A., Pham, Q.B. and Tiefenbacher, J.P. (2022b). Evaluating novel hybrid models based on GIS for snow avalanche susceptibility mapping: A comparative study. *Cold Regions Science and Technology*, 194, p.103453. <https://doi.org/10.1016/j.coldregions.2021.103453>
- Yariyan, P., Feizizadeh, B., Blaschke, T., Yakar, M., & Karimzadeh, S. (2026). Integrating environmental predictors and deep learning approach for spatiotemporal dust storm risk mapping and impacts modeling on land, health and food security. *International Journal of Digital Earth*, 19(1), 2654262. <https://doi.org/10.1080/17538947.2026.2654262>